

5 Results

5.1 Characterization of *Ext1*^{Gt/Gt} Mice

To analyze the role of *Ext1* dependent heparan sulfate (HS) during endochondral ossification, we investigated a mouse line mutant for *Ext1* (*Ext1*^{Gt/Gt}), which was generated in a gene trap screen. This screen was carried out with a modified gene-trap strategy to isolate insertional mutations specifically in secreted and membrane-spanning proteins. The trapped genes were identified by 5' RACE-PCR (Mitchell et al., 2001). In the *Ext1*^{Gt/Gt} mice, the gene trap vector (*PGT2Tm*pf_s, Fig. 8) (Leighton et al., 2001) has inserted into the first intron, creating a truncated *Ext1* protein fused to the β -*geo* reporter of the vector (Fig. 11 A). We performed inverse PCR to identify the exact insertion site within the 274 kb long intron. Genomic DNA was digested with either *Xba*I or *Bam*HI. The fragments were circularized and nested PCR was performed with primer pairs located at the distal ends of the gene trap vector (Fig. 8). Only circularized fragments, derived from the *Bam*HI digest, gave amplification products after the second round of PCR. These were cloned, sequenced and blasted against the mouse genome (NCBI). The identified sequences aligned with contig NT_078782.1 on mouse chromosome 15 and the position of the insertion site was determined to be 48 kb downstream of exon1 of *Ext1*. The identification of the insertion site confirmed targeting of *Ext1* and allowed the design of a PCR-strategy for genotyping *Ext1*^{Gt/Gt} mice.

Homozygous *Ext1*^{Gt/Gt} embryos survive until E14.5 at a nonmendelian ratio of 14%, 6% survive until E15.5 and only 4% can be recovered at E16.5. *Ext1*^{Gt/Gt} embryos are small and appear edematous (Fig. 9A,B). Heart defects are a likely cause for the embryonic lethality: sections of mutant embryos at E14.5 reveal reduced cardiac muscles and a failure to septate the outflow tract and ventricular chambers (O.G.Kelly and W.C. Skarnes, unpublished data). Alcian blue staining revealed a reduced skeleton size with fused vertebrae, shortened fore- and hindlimbs, fusions of elbow and knee joints, and occasionally syndactylies of digits (Fig. 9 C-H). As targeted deletion of *Ext1* (*Ext1*^{-/-}) is lethal during gastrulation (Lin et al., 2000), the insertion of the gene trap vector in *Ext1*^{Gt/Gt} mice seems to create a hypomorphic allele of *Ext1*.

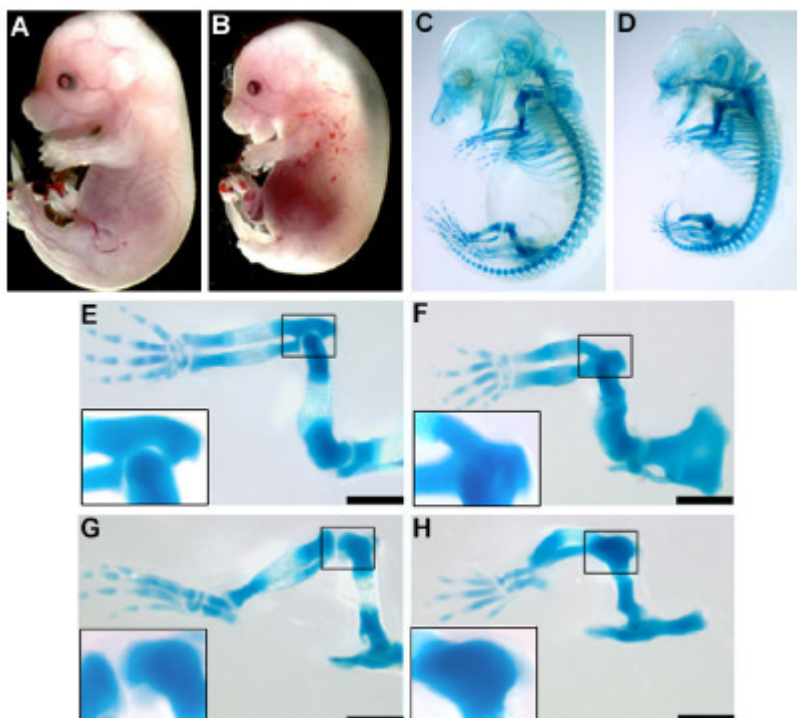


Fig. 9. Phenotype of *Ext1*^{Gt/Gt} mice. (A,B) E15.5 *Ext1*^{Gt/Gt} mice (B) are small and edematous. (C-H) Alcian blue staining of E15.5 *Ext1*^{Gt/Gt} embryos (D) reveals short skeletal elements and fused vertebrae. Fore- (E,F) and hindlimbs (G,H) show fusions in elbow and knee joints in *Ext1*^{Gt/Gt} mice (F, H). Scale bars: 250 μ m.

5.2 *Ext1*^{Gt/Gt} mice synthesize reduced amounts of HS

To test if HS synthesis is disturbed in *Ext1*^{Gt/Gt} mice, we stained sections of E14.5 limbs with the anti-HS-antibody 3G10, which detects unsaturated glucuronate at the nonreducing ends of HS chains after digestion with heparatinase (David et al., 1992). Interestingly, reduced but significant amounts of HS can be detected in *Ext1*^{Gt/Gt} mice (Fig. 10). In contrast, no HS is synthesized in *Ext1*^{-/-} mice (Lin et al., 2000), confirming that the gene trap insertion results in a hypomorphic allele of *Ext1*.

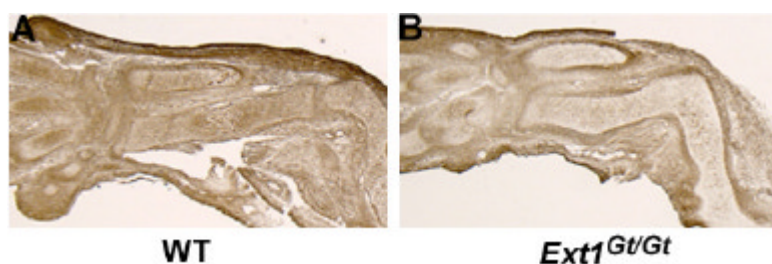


Fig. 10. Reduced amounts of HS in in *Ext1^{Gt/Gt}* mice. Immunohistochemistry with the 3G10 antibody on limb sections of E14.5 wild-type mice (A) detects high levels of ubiquitously distributed HS (brown staining), which are reduced in *Ext1^{Gt/Gt}* mice (B).

To test if expression of full-length protein contributes to the residual glycosyltransferase activity, we analyzed wild-type and mutant *Ext1* mRNA by RT-PCR. If the splice acceptor of the gene trap vector is skipped at a low rate, low levels of full length transcript should be detectable. Primer pairs, designed to detect the full-length transcript, were used to amplify different DNA fragments from exon 6 to exon 9. Indeed the mutant cDNA template revealed a specific amplification product after 28 PCR-cycles. However the amount of amplified cDNA was severely reduced compared to the amplified transcript of the wild-type cDNA (Fig. 11 B).

To quantify the amount of full-length transcript in the *Ext1^{Gt/Gt}* mutant we performed Real Time PCR (Fig. 11 C and D). Using primer pairs specific either for the wild-type (exon1/exon2 and exon7/exon8) or for the mutant allele (exon1/gene trap vector), we found that heterozygous *Ext1^{Gt/+}* mice transcribe each allele in equal amounts of 50%. In contrast, homozygous *Ext1^{Gt/Gt}* mice transcribe about 3% of wild-type *Ext1* mRNA (n = 2). It is thus likely that alternative splicing around the gene trap vector results in low amounts of wild-type Ext1 protein in *Ext1^{Gt/Gt}* mice, resulting in sufficient enzyme activity allowing survival of *Ext1^{Gt/Gt}* mice until E16.5.

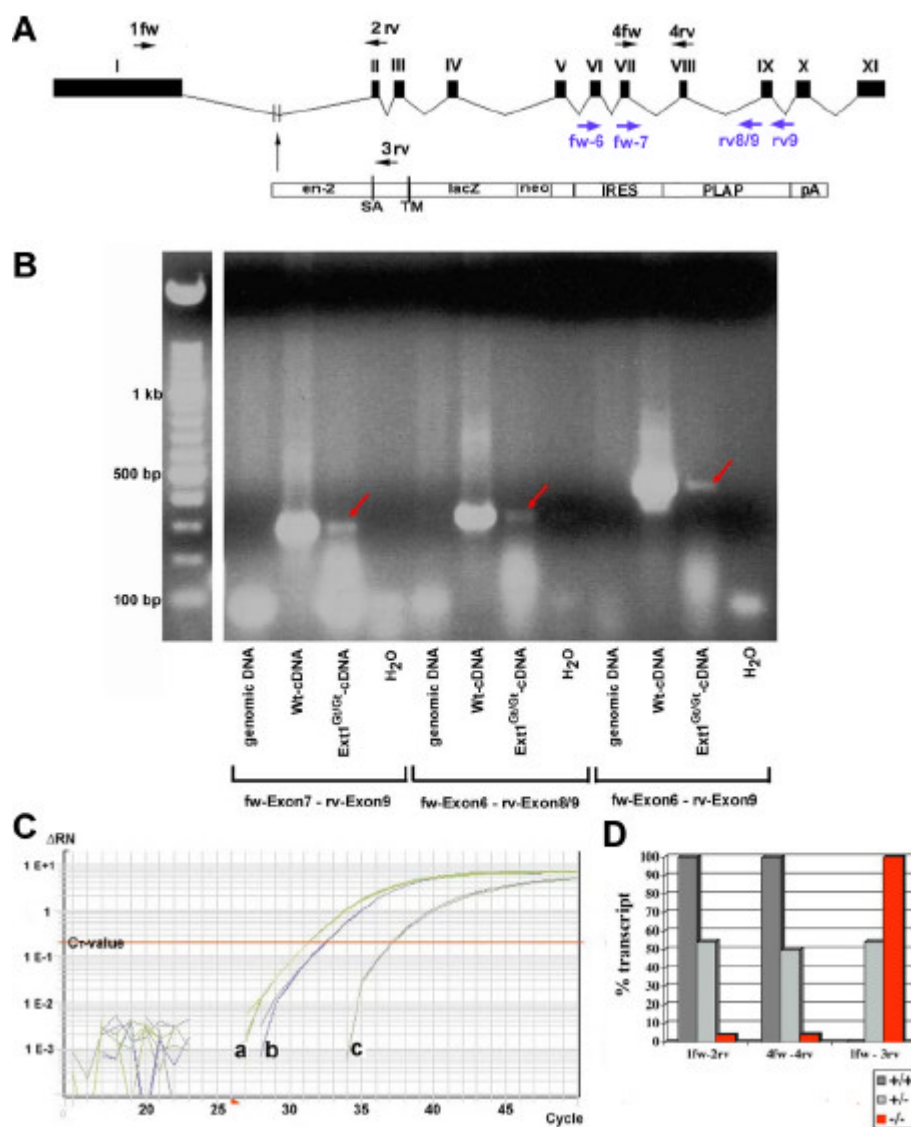


Fig. 11. *Ext1*^{Gt/Gt} mice display a hypomorphic allele of *Ext1*. (A) Schematic representation of the *Ext1* gene and the gene trap vector. (B) RT-PCR of different transcripts (exon 7 to exon 9, exon 6 to exon 8/9, exon 6 to exon 9) from wild-type and *Ext1*^{Gt/Gt} cDNA (primer pairs are indicated as blue arrows in (A)). Low levels of amplification product from mutant cDNA are detectable after 28 PCR-cycles (red arrows). (C, D) Quantification of *Ext1* transcripts. Primer pairs used for quantitative RT-PCR are indicated as black arrows in (A). (C) Amplification plot of a PCR run with the primer pairs 1fw-2rv, showing the increase of fluorescence emission (ΔRN) correlated to the number of PCR-cycles. The amplification product of the wild-type cDNA (a) reaches the threshold value (C_T -value) one cycle earlier than the *Ext1*^{Gt/+} cDNA (b) and about 5 cycles earlier than the *Ext1*^{Gt/Gt} cDNA (c). (D) Quantification of transcript levels: heterozygous *Ext1*^{Gt/+} mice express around 50% full-length wild-type (fw1-rv2, fw4-rv4) and 50% *Ext1* gene trap transcript (fw1-rv3). Homozygous *Ext1*^{Gt/Gt} mice express 3% wild-type transcript (n = 2).

5.3 *Ext1*^{Gt/Gt} mice show delayed hypertrophic differentiation

To investigate the role of *Ext1* during bone development, we analyzed cartilage morphology after Safranin Weigert (SW) staining in radius and ulna of wild-type and mutant forelimbs. At E14.5, wild-type embryos display well-organized zones of proliferating and hypertrophic chondrocytes. In contrast, *Ext1*^{Gt/Gt} mutants reveal joint fusions and a severe but highly variable delay in hypertrophic differentiation (Fig. 12 A, B). *In situ* hybridization revealed that *Ihh* is expressed in two domains of prehypertrophic chondrocytes, which flank a domain of *CollagenX* (*Col10a1*) expressing hypertrophic chondrocytes in wild-type embryos. In contrast, limbs of *Ext1*^{Gt/Gt} mutants show only weak expression of *Ihh* in the center of the cartilage elements and *Col10a1* is not expressed in most mutants at E14.5 (Fig. 12A–D). Impaired chondrocyte differentiation and a severely reduced region of *Ihh*-expressing cells can already be detected at E13.5 in *Ext1*^{Gt/Gt} mutants (data not shown). As strongly affected mutants often lose their elbow joints before E14.5, *Pthlh* expression was shifted to the outside of the continuous skeletal elements (Fig. 12 J, red arrow). Similar expression patterns were observed with *growth differentiation factor-5* (*Gdf5*) (data not shown). Expression of this early joint marker was, however, detectable in the joints of carpals and digits of *Ext1*^{Gt/Gt} limbs, indicating that joint formation is not perturbed in general. Loss of joints in these mutants most likely occurs secondarily due to the overproliferation of chondrocytes.

In comparison to the majority of embryos at younger stages, *Ext1*^{Gt/Gt} mutants at E15.5 and E16.5 display a milder, albeit more stable, phenotype, presumably because less-affected mutants survive longer. SW staining reveals short and broad skeletal elements with expanded zones of proliferating chondrocytes and severely delayed bone formation (Fig. 13 A, B). Additionally the shape of chondrocytes is different: Proliferating chondrocytes next to the hypertrophic region, which are normally organized in columns of flattened cells, appear round and disorganized in *Ext1*^{Gt/Gt} mutants (Fig. 13 C, D).

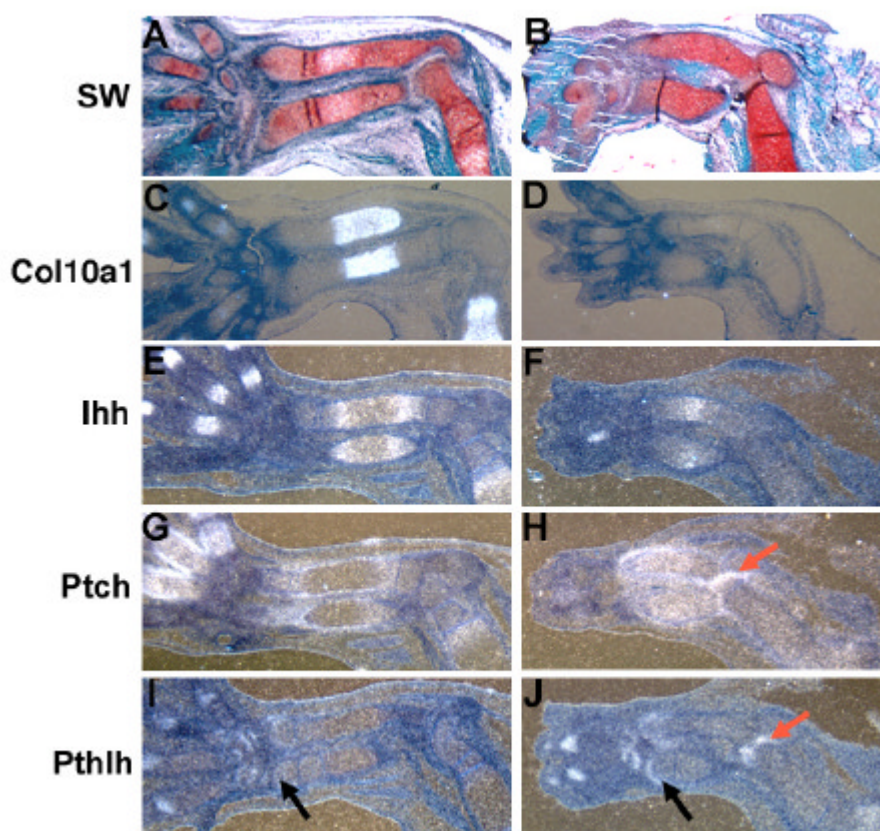


Fig. 12. Early limb development is disturbed in *Ext1^{Gt/Gt}* mice. Sections of E14.5 wild-type and *Ext1^{Gt/Gt}* mutant limbs were stained with Safranin Weigert (SW) or hybridized with antisense riboprobes as indicated. E-J display parallel sections. (A,B) At E14.5, SW staining reveals severely delayed cartilage development. (C-J) Whereas the zone of *Ihh* expression (E) has split into two domains flanking the expression domain of *Col10a1* in wild-type embryos (C), *Ext1^{Gt/Gt}* mice display a small continuous *Ihh* expression domain (F) and do not express *Col10a1* (D). Nevertheless, *Ptch* expression is strongly upregulated throughout the cartilage anlagen (G and H). Similarly, the expression of *Pthlh* is upregulated in *Ext1^{Gt/Gt}* mutants (I and J, black arrow). Note the coexpression of strong *Pthlh* and *Ptch* expression in the elbow joint (red arrow).

In E15.5 and E16.5 *Ext1^{Gt/Gt}* mutants, the zone of *Ihh* expression is reduced (Fig. 14 and Fig. 16). Markers for hypertrophic chondrocytes, *Col10a1* and *Matrix-metalloprotease-13* (*Mmp13*), are expressed in distinct domains similar to wild-type embryos (Fig. 14 C-F). However, the hypertrophic region is not separated by endochondral bone in *Ext1^{Gt/Gt}* mutants as shown by lack of expression of the osteoblast marker *osteocalcin* (*bone gla protein1*, *Bglap1*) (Fig. 14 G, H).

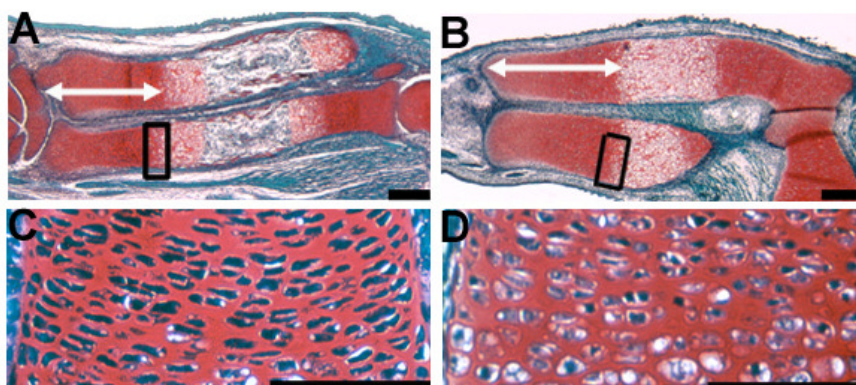


Fig. 13. Cartilage morphology of E16.5 wild-type (A,C) and *Ext1*^{Gt/Gt} mutant (B, D) limbs. Sections were stained with Safranin Weigert (SW). At E16.5 *Ext1*^{Gt/Gt} mice show an enlarged zone of proliferating chondrocytes (white arrow) and terminal hypertrophic chondrocytes have not been replaced by bone. (C,D) Higher magnification of proliferating chondrocytes marked in (A) and (B). The organization of chondrocytes is irregular and column formation is disturbed in *Ext1*^{Gt/Gt} mice. Scale bars: 250 μ m (A,B); 100 μ m (C,D).

No significant alteration in the expression of either *Runx2* or *Runx3*, two positive regulators of chondrocyte and osteoblast differentiation, could be detected in *Ext1*^{Gt/Gt} mutants (Fig. 14 I, J and data not shown). Since *Bglap1* and *Runx2* expression is maintained in the periosteum in *Ext1*^{Gt/Gt} mutants, the lack of endochondral bone is not due to impaired osteoblast differentiation, but rather reflects the delay in chondrocyte differentiation.

In the *Ext1*^{Gt/Gt} mice other bones, formed by endochondral ossification, like ribs and vertebrae, are also severely affected. Hematoxylin-Eosin staining of ribs and vertebrae of E15.5 embryos revealed disturbed chondrocyte and bone differentiation in these skeletal elements. Similar as in limbs, mutant ribs show disorganized proliferating chondrocytes and a failure to replace hypertrophic chondrocytes with endochondral bone. The cartilaginous vertebral bodies are fused, indicating increased chondrocyte proliferation (Fig. 15 E, F). In contrast to *Ext1*^{Gt/Gt} mice, we could not detect a skeletal phenotype in *Ext1*^{Gt/+} embryos.

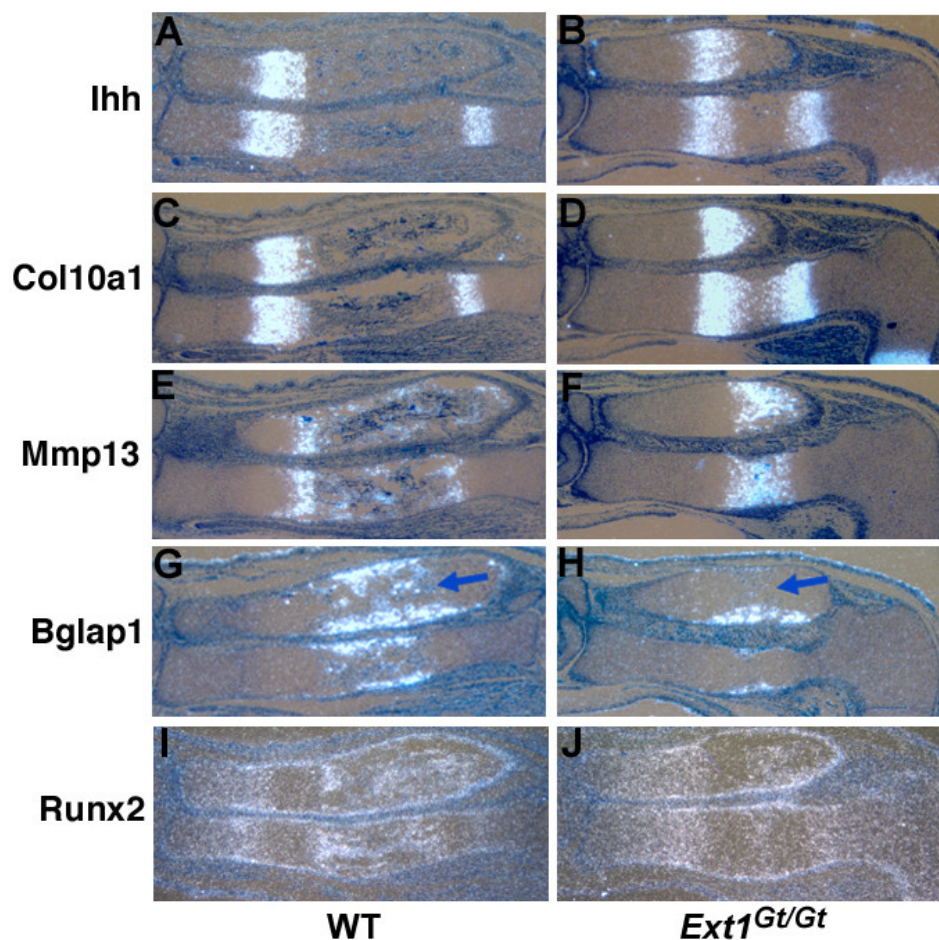


Fig. 14. Hypertrophic differentiation is delayed in *Ext1^{Gt/Gt}* mice. E16.5 limb sections were hybridized with antisense riboprobes as indicated. (A-H) display parallel sections. (A, B) *Ext1^{Gt/Gt}* mice show reduced expression of *Ihh*. (C-F) Central chondrocytes have differentiated into hypertrophic and terminal hypertrophic chondrocytes expressing *Col10a1* and *Mmp13*, respectively. (G, H) No bone formation can be detected in the center of the developing skeletal elements in *Ext1^{Gt/Gt}* mutants as seen by the lack of *Bglap1* expression (blue arrow). (I, J) *Runx2* is expressed in normal pattern.

5.4 *Pthlh* and *Ptch* are upregulated in *Ext1^{Gt/Gt}* embryos

A reduced level of *Ihh* expression in *Ext1^{Gt/Gt}* mice would be expected to accelerate the onset of hypertrophic differentiation. Instead, the expanded distance between the *Ihh* expression domain and the joint region in E16.5 mutant embryos indicates a severe delay in the onset of hypertrophic differentiation. *Pthlh* is the effective molecule downstream of *Ihh* signaling in regulating the onset of hypertrophic differentiation. Surprisingly, at all stages analyzed, *Pthlh* expression is upregulated in *Ext1^{Gt/Gt}* mutants (Fig. 12 and Fig. 16).

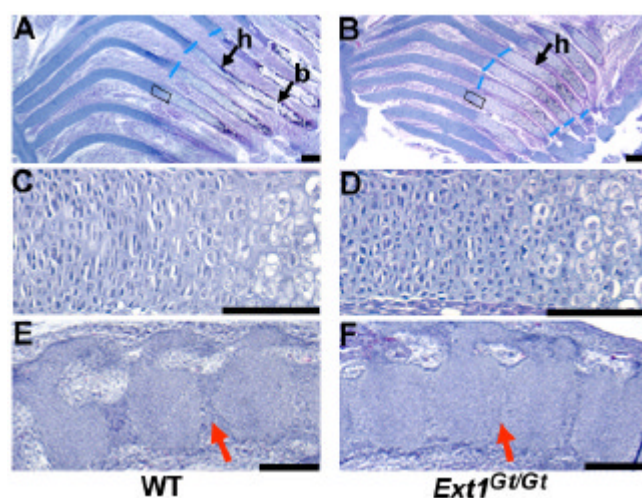


Fig. 15. Endochondral ossification of ribs and vertebrae. Hematoxylin/ Eosin staining of sagittal sections of ribs and vertebrae. (A, B) Ribs of *Ext1^{Gt/Gt}* mice show delayed endochondral ossification (blue bar, border of hypertrophic chondrocytes (h); b, bone). (C, D) Higher magnification of insets in (A) and (B) show disorganized proliferating chondrocytes in *Ext1^{Gt/Gt}* mice. (E, F) Vertebrae are enlarged and individual elements are fused in *Ext1^{Gt/Gt}* mice (red arrow).

Upregulation of *Pthlh* expression despite reduced amounts of *Ihh* could indicate that other growth factors regulate *Pthlh* expression independent of *Ihh*. Alternatively, *Ihh* signaling might be potentiated by the reduced amounts of HS in *Ext1^{Gt/Gt}* mutants. To test the latter, we examined the expression of *Patched* (*Ptch*), which is upregulated in all cells receiving a Hedgehog signal (Goodrich et al., 1996). In *Ext1^{Gt/Gt}* mutant mice, *Ptch* expression is upregulated in most embryos at E14.5 (Fig. 12 G, H). Only strongly affected embryos expressing no or significantly reduced amounts of *Ihh* show reduced expression of *Ptch* compared to wild-type embryos (data not shown). Interestingly, in a subset of mutants, strong *Ptch* expression is detected overlapping with upregulated *Pthlh* expression (Fig. 12 H, J).

At E15.5 and E16.5, two domains of *Ptch* expression can be distinguished at the distal ends of ulna and radius of wild-type limbs: a domain of strong *Ptch* expression in chondrocytes adjacent to the *Ihh*-expressing cells, and a domain of weaker *Ptch* expression at the distal ends of the cartilage elements, which encompasses the *Pthlh* expressing periarticular cells. In *Ext1^{Gt/Gt}* mutants, the region of strong *Ptch* expression is expanded toward the joint region (Fig. 16 C, D, G). This difference is more significant if the domain of strong *Ptch* expression is related to the domain of *Ihh*-expressing cells (60% increase,

Fig. 16 H). As *Ptch* expression can be used as readout for *Ihh* signaling, the broader domain of high *Ptch* expression strongly indicates an increased range of *Ihh* signaling in *Ext1^{Gt/Gt}* mutants.

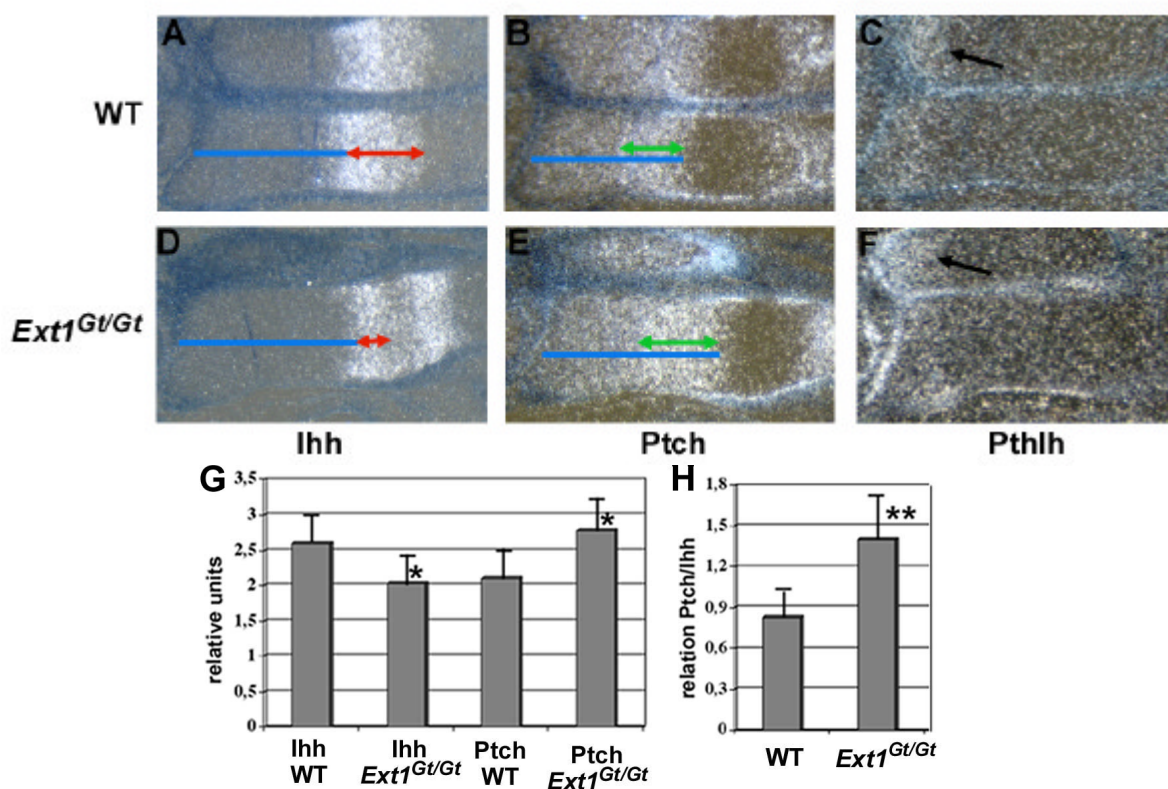


Fig. 16. Range of *Ptch* expression is increased in *Ext1^{Gt/Gt}* mice. (A–F) *In situ* hybridization on serial sections of E15.5 wild-type and *Ext1^{Gt/Gt}* mutant limbs revealed a reduced expression domain of *Ihh* (A, B, red arrow) whereas the domain of strong *Ptch* expression is increased (B, E, green arrow). (G) Relative sizes of *Ihh* and *Ptch* expression domains ($n = 14$, *: $p < 0.02$, unpaired student's t test). (H) The domain of *Ptch* expression in relation to the *Ihh* expression domain is increased by 60% ($n = 14$, **: $p < 0.01$, unpaired student's t test). (C, F) *Pthlh* expression is upregulated in *Ext1^{Gt/Gt}* mice (black arrow).

5.5 *Ihh* distribution is extended in *Ext1^{Gt/Gt}* mice

The extended range of *Ihh* signaling in *Ext1^{Gt/Gt}* mice suggests that reduced levels of HS alter the propagation of *Ihh* protein. To test this hypothesis, we analyzed the distribution of *Ihh* protein by immunohistochemistry using the Shh antibody, ShhAb80 (Yang et al., 1997), which crossreacts with *Ihh* protein (Gritli-Linde et al., 2001). At E15.5

and E16.5, ShhAb80 detects a gradient of Ihh protein that extends from the Ihh-expressing chondrocytes into the adjacent region of proliferating cells (Fig. 17 I and 3J). To analyze the distribution of Ihh protein in relation to its expression domain, we determined the distal border of Ihh mRNA expression in controlateral limbs. Using this border as start point, we measured the distance, in which we could detect Ihh protein. We found extended domains of detectable Ihh protein in the proliferating chondrocytes in *Ext1^{Gt/Gt}* mutants (n = 4) (Fig. 17). Similar to the expression of *Ptch*, this difference is more evident if the domain of Ihh protein is analyzed in relation to the Ihh expression domain. Together, these data strongly indicate that reduced amounts of HS in *Ext1^{Gt/Gt}* embryos facilitate the distribution of Ihh protein. Consequently, the delayed onset of hypertrophic differentiation in *Ext1^{Gt/Gt}* mice might be due to an activated Ihh signal.

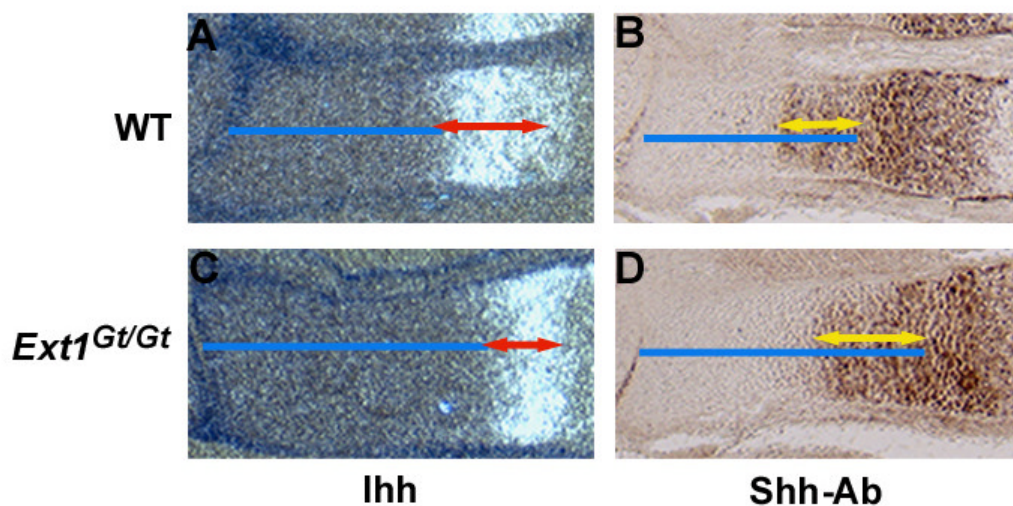


Fig. 17. The range of Ihh is extended in *Ext1^{Gt/Gt}* mice. ShhAb80 immunohistochemistry reveals an extended domain of detectable Ihh protein in proliferating chondrocytes (B, D, yellow arrow). The distal border of the *Ihh* expression domain, which was identified by *in situ* hybridization with an *Ihh* riboprobe on controlateral limbs (A, C), was used as a reference (blue line) (n = 4).

5.6 Block of Ihh signaling rescues the delayed onset in hypertrophic differentiation in *Ext1^{Gt/Gt}* mice

To support the idea that increased Ihh signaling leads to the delayed onset of hypertrophic differentiation in *Ext1^{Gt/Gt}* mice, we attempted to inhibit Ihh signaling. The

alkaloid cyclopamine specifically inhibits the *Ihh* signaling pathway in limb explant cultures (Minina et al., 2001). Treatment of wild-type limbs with cyclopamine results in a block of *Ptch* and *Pthlh* expression and in an accelerated onset of hypertrophic differentiation. Similar to wild-type limb explants, treatment of E15.5 *Ext1^{Gt/Gt}* limbs with cyclopamine results in a block of *Ptch* and *Pthlh* expression (Fig. 18 E, F, K, L). Furthermore, the onset of hypertrophic differentiation is accelerated in *Ext1^{Gt/Gt}* limbs, as indicated by a reduced distance between the *Ihh* expression domain and the joint region (A, D, G, J, red arrow). As inhibition of *Ihh* signaling can rescue the delay in hypertrophic differentiation, increased *Ihh* signaling seems to be responsible for the *Ext1^{Gt/Gt}* phenotype.

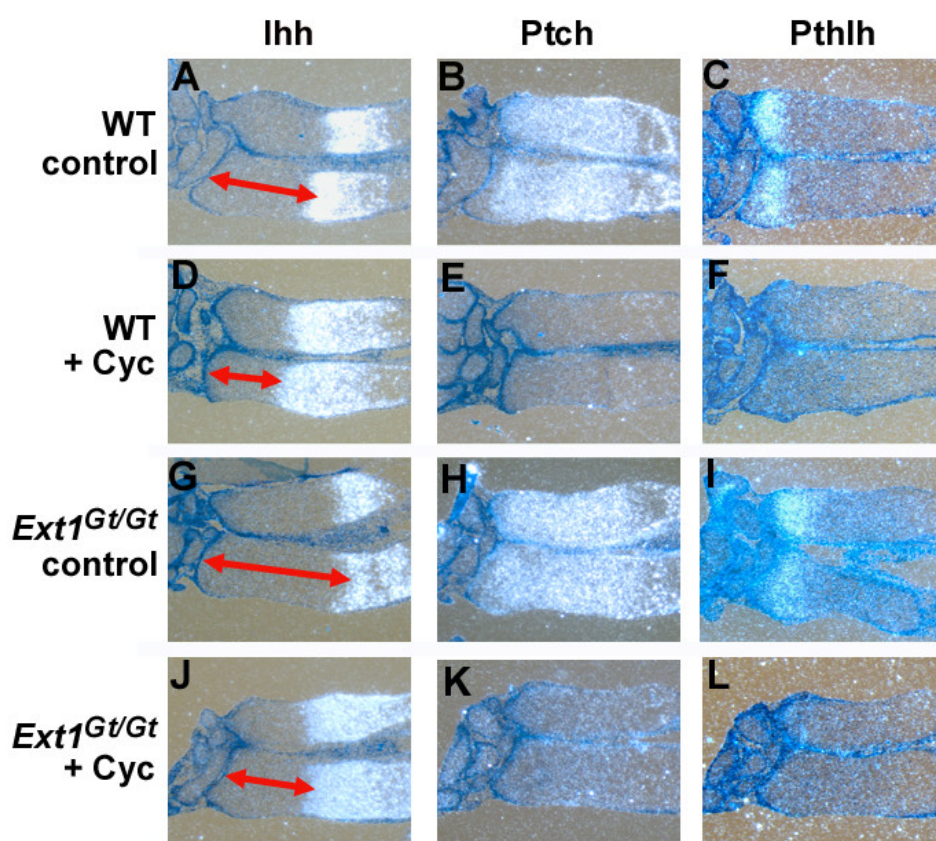


Fig. 18. *Ihh* acts downstream of *Ext1*. Forelimbs of E15.5 wild-type (A–F) and *Ext1^{Gt/Gt}* (G–L) mouse embryos were cultured for 2 days with control medium (A–C and G–I) or medium supplemented with cyclopamine (D–F and J–L). Serial sections were hybridized with antisense riboprobes as indicated. Wild-type and *Ext1^{Gt/Gt}* limbs show accelerated hypertrophic differentiation, which leads to a reduced distance between the *Ihh* expression domain and the joint region (A, D, G, J, red arrow). Neither *Ptch* nor *Pthlh* expression can be detected after treatment with cyclopamine.

5.7 Chondrocyte proliferation is increased in the periarticular region of *Ext1*^{Gt/Gt} mice

In addition to its role in regulating chondrocyte differentiation, *Ihh* signaling activates chondrocyte proliferation, independent of *Pthlh* (St-Jacques et al., 1999). The region of proliferating chondrocytes can be subdivided into a zone of low-proliferating, periarticular chondrocytes (zone I) and a zone of high-proliferating, columnar chondrocytes (zone II) (Long et al., 2001). Chondrocytes in zone I have a round morphology, whereas chondrocytes of zone II are flattened and arranged in columns orientated longitudinally. We determined the proliferation rate in defined regions of each zone in radii of wild-type, *Ext1*^{Gt/+}, and *Ext1*^{Gt/Gt} embryos at stage E15.5 (Fig. 19). We found no statistically significant differences of chondrocyte proliferation in zone II (20%–24%). In contrast, the proliferation rate in zone I is increased from 12% in wild-type and *Ext1*^{Gt/+} mice to 19% in *Ext1*^{Gt/Gt} embryos. The increased proliferation rate in zone I of the *Ext1*^{Gt/Gt} mutants is in accordance with an extended range of *Ihh* signaling.

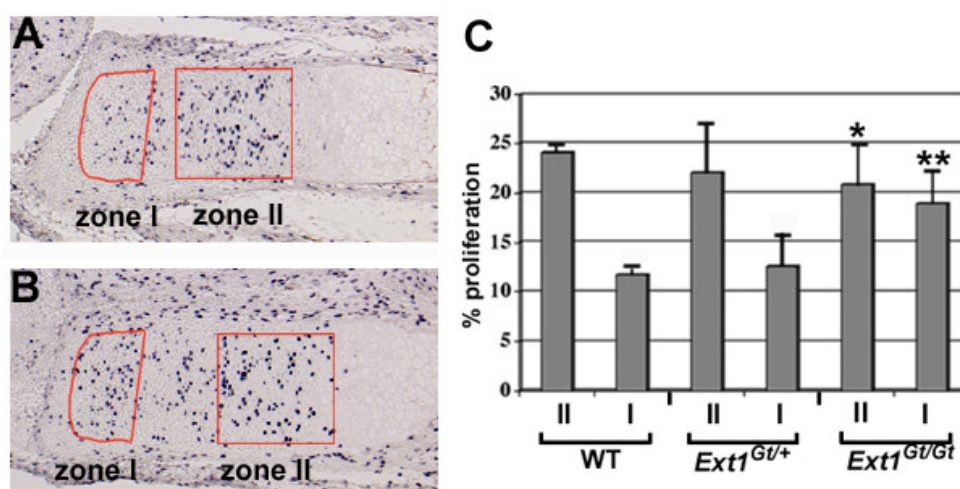


Fig. 19. Chondrocyte proliferation is upregulated in periarticular chondrocytes in *Ext1*^{Gt/Gt} mice. Proliferating cells were labeled with BrdU, detected by antibody staining, and analyzed in defined regions of wild-type, *Ext1*^{Gt/+} and *Ext1*^{Gt/Gt} mice at E15.5 (A, B and data not shown). (C) Proliferation rates in zone II are similar in all three genotypes (n = 4, *: p > 0.05 unpaired student's t test), whereas zone I of *Ext1*^{Gt/Gt} mutants shows an increased proliferation rate of 19% compared to 12% in wild-type mice (n = 4, **: p < 0.02 unpaired student's t test).

5.8 Ectopic HS restrict *Ihh* signaling

Our results so far suggest that reduced amounts of HS in *Ext1^{Gt/Gt}* mice lead to an increased range of *Ihh* signaling. Consequently, increased HS concentrations should restrict *Ihh* signaling and accelerate the onset of hypertrophic differentiation. To test this hypothesis, we treated limb explants of E15.5 wild-type embryos in culture with ectopic HS, heparin, or chondroitin sulfate (CS) for 2 days (Fig. 20). Treatment of limbs with 1 $\mu\text{g/ml}$, 10 $\mu\text{g/ml}$, or 100 $\mu\text{g/ml}$ HS leads to an accelerated onset of hypertrophic differentiation in a dose-dependent manner (Fig. 20 A, D, G). Hence the induced changes in HS-treated limbs are analog to the accelerated onset of hypertrophic differentiation seen after cyclopamin treatment. To explore the range of *Ihh* signaling after treatment with HS, we analyzed the expression of *Ptch*. Strikingly, in limbs treated with high concentrations of HS, *Ptch* expression is restricted to a narrow stripe of chondrocytes directly adjacent to the *Ihh* expression domain and to the flanking peric hondrium/periosteum (Fig. 20 B, E, H). No expression of *Ptch* could be detected in distal chondrocytes. Similar results were obtained after treatment with heparin (Fig. 20 J–L). Interestingly, heparin, which is more highly sulfated, is more effective in restricting the *Ihh* signal, indicating that not only the amount of HS but also the degree of sulfation might be critical to determine the range of the *Ihh* signal. In contrast, treatment with CS does not inhibit *Ptch* expression, supporting the specificity of HS for binding *Ihh*.

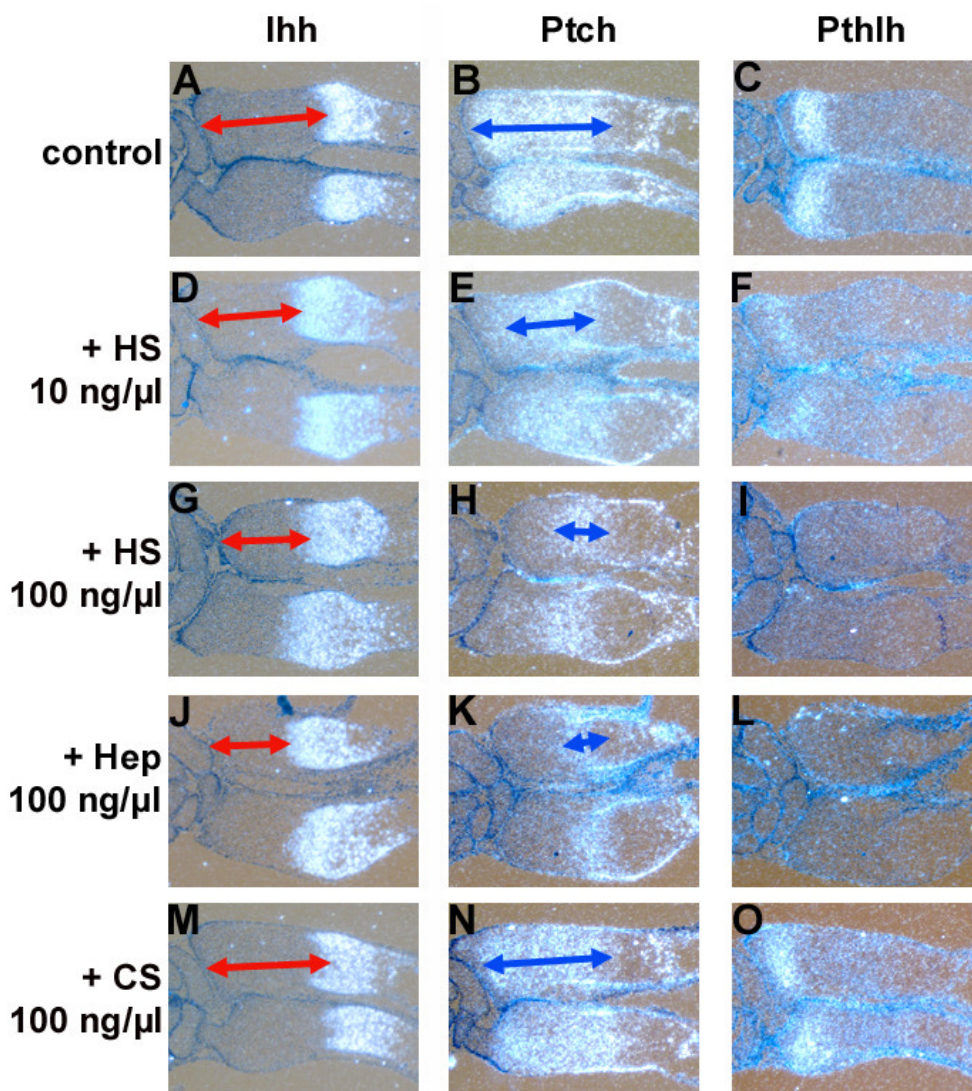


Fig. 20. Ectopic HS restrict *Ihh* signaling. Forelimbs of E15.5 wild-type mouse embryos were cultured for 2 days in control medium (A–C) or in medium supplemented with HS (D–I), heparin (Hep) (J–L), or chondroitin sulfate (CS) (M–O). Serial sections were hybridized with antisense riboprobes as indicated. Treatment of wild-type limbs with HS and heparin leads to a reduced distance between the *Ihh* expression domain and the joint region (red arrow). HS and heparin restrict *Ptch* expression (blue arrow) to the *Ihh* expression domain in a concentration-dependent manner (B, E, H, and K). Similarly, *Pthlh* expression is reduced in a concentration-dependent manner by HS and heparin (C, F, I, and L). (M–O) Treatment with CS does not effect *Ptch* (N) or *Pthlh* expression (O).

We furthermore treated limb explants of E15.5 *Ext1^{Gt/Gt}* mice with HS, heparin, and CS. As in wild-type limbs, we observed a dose-dependent acceleration of the onset of hypertrophic differentiation with HS and heparin, whereas CS has no effect (Fig. 21 and

data not shown). Similar to cyclopamine, HS supplementation thus rescues the *Ext1^{Gt/Gt}* phenotype. Together these results support the hypothesis that reduced amounts of HS are responsible for the delay in chondrocyte differentiation in *Ext1^{Gt/Gt}* mice

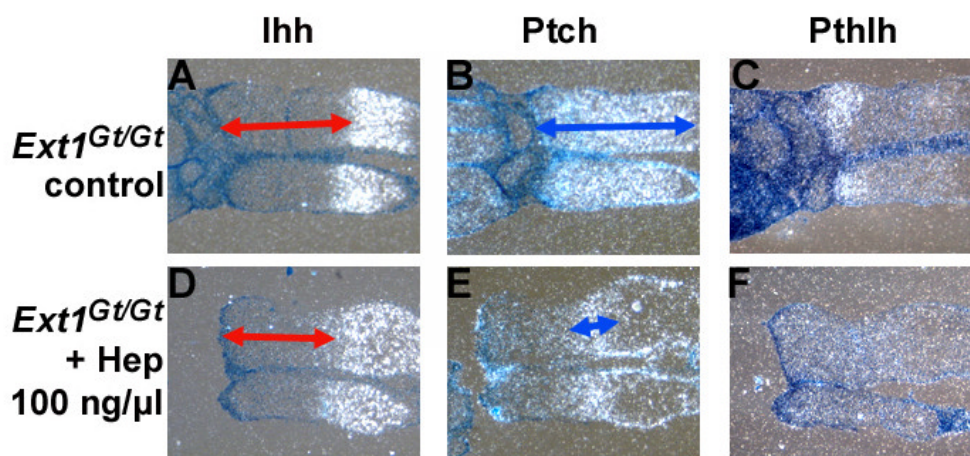


Fig. 21. Heparin treatment rescues the onset of hypertrophic differentiation in *Ext1^{Gt/Gt}* limbs. Forelimbs of E15.5 *Ext1^{Gt/Gt}* limbs were cultured for 2 days in control medium (A–C) or in medium supplemented with heparin (Hep) (D–F). Serial sections were hybridized with antisense riboprobes as indicated. The expression of *Ptch* (B, E) and *Pthlh* (C, F) is reduced in *Ext1^{Gt/Gt}* mutant limbs after heparin treatment.

5.9 Regulation of *Pthlh* expression

As explained above, it has not yet been resolved whether *Ihh* directly or indirectly regulates *Pthlh* expression. After HS treatment, cells adjacent to the *Ihh* expression domain still react to *Ihh* signals by upregulating *Ptch* expression and should thus be able to produce secondary signals. Surprisingly, we found severely reduced expression of *Pthlh* in the periarticular region after treatment with heparin or HS in a dose-dependent manner, implicating a direct regulation of *Pthlh* expression by the *Ihh* signal (Fig. 20 C, F, I, L). In contrast, treatment with CS does not alter the expression of *Pthlh*. Similar results were obtained after treatment of *Ext1^{Gt/Gt}* mutant limbs.

Bmps and Tgfs have long been hypothesized to act as secondary signals downstream of *Ihh* to induce the expression of *Pthlh* (Alvarez et al., 2002; Zou et al., 1997). Previously, Bmps were excluded from acting as such mediators (Minina et al., 2001). To further support a direct regulation of *Pthlh* by *Ihh*, we have treated limb explants of E15.5 and E16.5 embryos with Tgfb1. We detected no significant alteration in *Pthlh* expression. The

alkaloid cyclopamine inhibits *Ihh* signaling in limb culture, leading to a block of *Pthlh* expression. Importantly, cotreatment of limb explants with cyclopamine and Tgfb1 could not rescue the expression of *Pthlh* (Fig. 18 D, F, and Fig. 22). We can thus exclude Tgfb1 as a secondary signal inducing *Pthlh* expression downstream of *Ihh*. Together, these data strongly suggest that *Ihh* directly activates the expression of *Pthlh* independent of secondary factors.

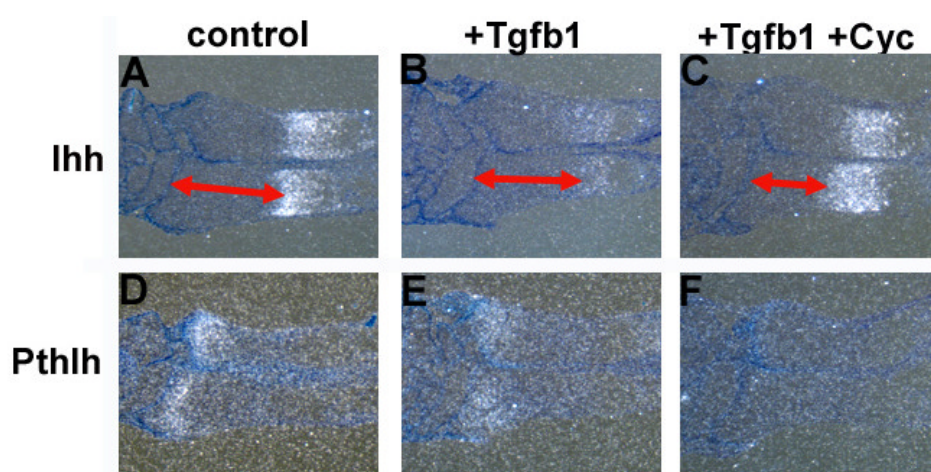


Fig. 22. Tgfb1 cannot activate *Pthlh* independent of *Ihh*. Forelimbs of E15.5 wild-type mice were cultured for 2 days in control medium (A, D) or treated with Tgfb1 (B, E) or Tgfb1 and cyclopamine (C, F) and hybridized with riboprobes as indicated. Treatment with Tgfb1 leads to a slightly accelerated onset of hypertrophic differentiation (A-C, red arrow). Tgfb1 cannot activate *Pthlh* expression independent of *Ihh* signaling (C-F).

To explore the mechanism, by which HS regulates *Ihh* signaling, we treated limb explants of mice overexpressing *Ihh* under the *Collagen2a1* (*Col2a1-Ihh*) (Long et al., 2001) with heparin. If HS only restrict *Ihh* distribution, treatment of *Col2a1-Ihh* limbs with high levels of heparin should have no effect on the expression of *Ptch* and *Pthlh*. As in untreated controls, we detected an upregulation of *Ptch* expression throughout the proliferating chondrocytes (Fig. 23). In addition *Pthlh* expression in the periarticular chondrocytes is unchanged. Thus treatment with high levels of heparin does not interfere with ligand-receptor binding. Therefore, HS seems to regulate *Ihh* signaling by restricting the distribution rather than by inhibiting the reception of the *Ihh* signal.

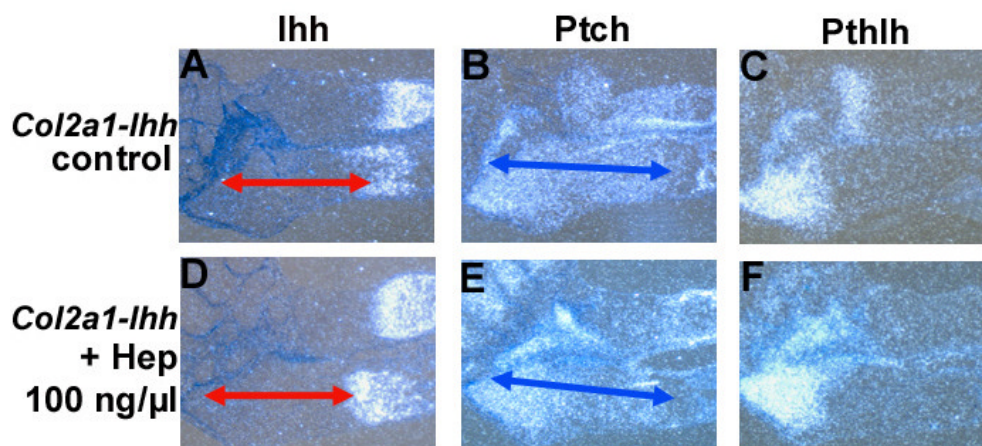


Fig. 23. Heparin treatment does not influence hypertrophic differentiation of *Ihh* overexpressing (*Col2a1-Ihh*) limb explants. Forelimbs of E15.5 *Col2a1-Ihh* limbs were cultured for 2 days in control medium (A–C) or in medium supplemented with heparin (Hep) (D–F). Serial sections were hybridized with antisense riboprobes as indicated. Both, *Ptch* (blue arrow in B, E) and *Pthlh* expression are not affected by treatment with heparin. In addition the onset of hypertrophic differentiation is unchanged in heparin treated *Col2a1-Ihh* limbs (red arrow in A, D).

5.10 Activated Fgf signaling does not rescue the delay in differentiation of *Ext1*^{Gt/Gt} mice

In vertebrates, Fgf signaling is dependent on an interaction between Fgf receptor, Fgf ligand, and HS (Esko and Selleck, 2002). The analysis of *Fgfr3*^{Ach/+} mice, which express a constitutively activated *Fgf receptor 3* (*Fgfr3*) under the *Col2a1* promoter, has shown that Fgf signaling reduces chondrocyte proliferation and accelerates the onset as well as the process of hypertrophic differentiation (Minina et al., 2002; Naski et al., 1998). Loss of Fgf signaling might thus contribute to the *Ext1*^{Gt/Gt} phenotype. To test if *Ext1*^{Gt/Gt} chondrocytes can respond to Fgf signals similar to wild-type chondrocytes, we treated E15.5 *Ext1*^{Gt/Gt} limb explants in culture with Fgf2 (Fig. 24 E–H). In both wild-type and *Ext1*^{Gt/Gt} explants, treatment with Fgf2 leads to reduced *Ihh* expression and a subsequent acceleration of the onset of hypertrophic differentiation, indicating that receptor binding is not disturbed in *Ext1*^{Gt/Gt} mutants. We further examined ligand-independent activation of Fgf signaling in *Ext1*^{Gt/Gt}; *Fgfr3*^{Ach/+} compound mutants. Interestingly, one allele of *Fgfr3*^{Ach/+} does not rescue the delayed onset of hypertrophic differentiation in *Ext1*^{Gt/Gt} mutants at E15.5 and E16.5 (Fig. 24 A–D). However, elbow and knee joints, which are always fused in *Ext1*^{Gt/Gt}

mutants, are partially rescued by activated Fgf signaling in *Ext1^{Gt/Gt};Fgfr3^{Ach/+}* mice (Fig. 24 D, red arrow). Therefore activation of Fgf signaling in *Ext1^{Gt/Gt}* mice may downregulate the proliferation rate. Thus joint fusions in *Ext1^{Gt/Gt}* limbs could develop secondary, caused by an increased proliferation rate of chondrocytes at the distal end of the skeletal elements near the joint forming region. In summary, Fgf signaling does not seem to be significantly disturbed in *Ext1^{Gt/Gt}* mice.

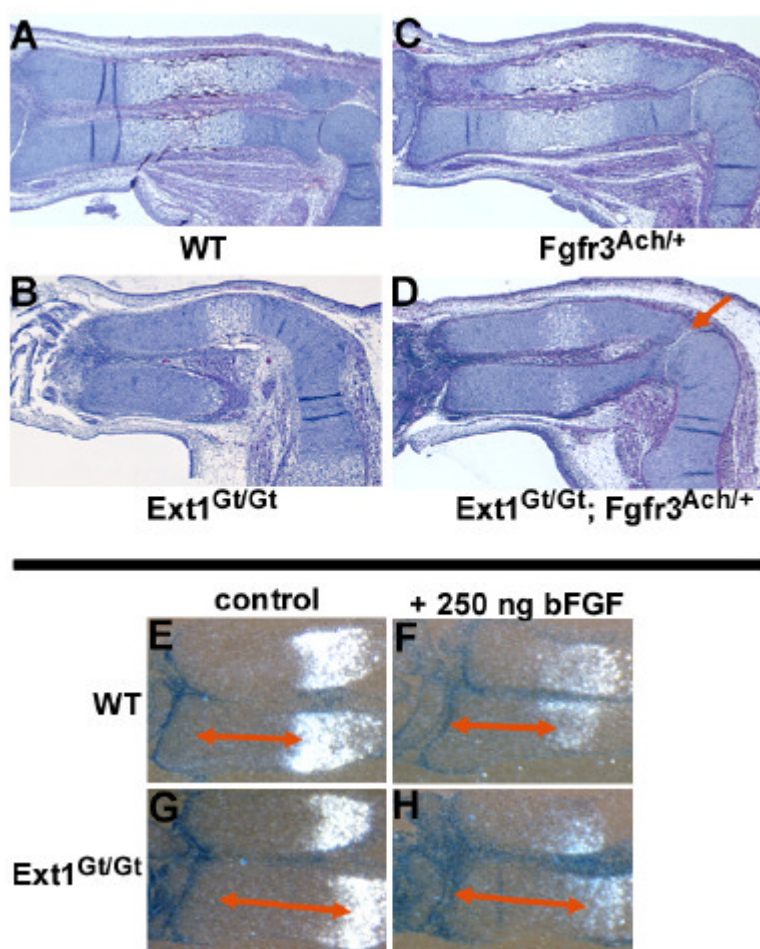


Fig. 24. Fgf signaling in *Ext1^{Gt/Gt}* mutants. (A–D) Hematoxylin/ Eosin staining of E15.5 wild-type (A), *Ext1^{Gt/Gt}* (B), *Fgfr3^{Ach/+}* (C), and *Ext1^{Gt/Gt}; Fgfr3^{Ach/+}* (D) limb sections. *Ext1^{Gt/Gt}; Fgfr3^{Ach/+}* mutants display a similar delay in hypertrophic differentiation as *Ext1^{Gt/Gt}* mutants; however, fusions of elbow joints are partially rescued (red arrow in D). (E–H) Forelimbs of E15.5 wild-type (E and F) or *Ext1^{Gt/Gt}* (G and H) mouse embryos were cultured for 2 days in control medium or medium supplemented with Fgf2. Serial sections were hybridized with an antisense riboprobe for *Ihh*. Limbs of wild-type and *Ext1^{Gt/Gt}* embryos react to Fgf treatment with reduced expression of *Ihh* and a subsequent accelerated onset of hypertrophic differentiation (red arrows).

5.11 Expression of the *Gli* gene family of transcription factors in the growth plate

During the process of endochondral ossification *Ihh* exerts three different functions: First it regulates hypertrophic differentiation through activation of *Pthlh* expression. Second *Ihh* positively regulates chondrocyte proliferation. Last not least *Ihh* induces bone collar formation in the perichondrium. It is not clear, how these different functions of *Ihh* are translated by the three transcription factors of the *Gli* gene family acting downstream of *Ihh*. To address this question we analysed the expression pattern of these genes in the developing growth plate. At E14.5 all three genes are expressed in the perichondrium surrounding the skeletal elements and in chondrocytes. *Gli2* and strong *Gli3* expression can additionally be detected in the joints and in mesenchymal cells surrounding the carpals (Fig. 25).

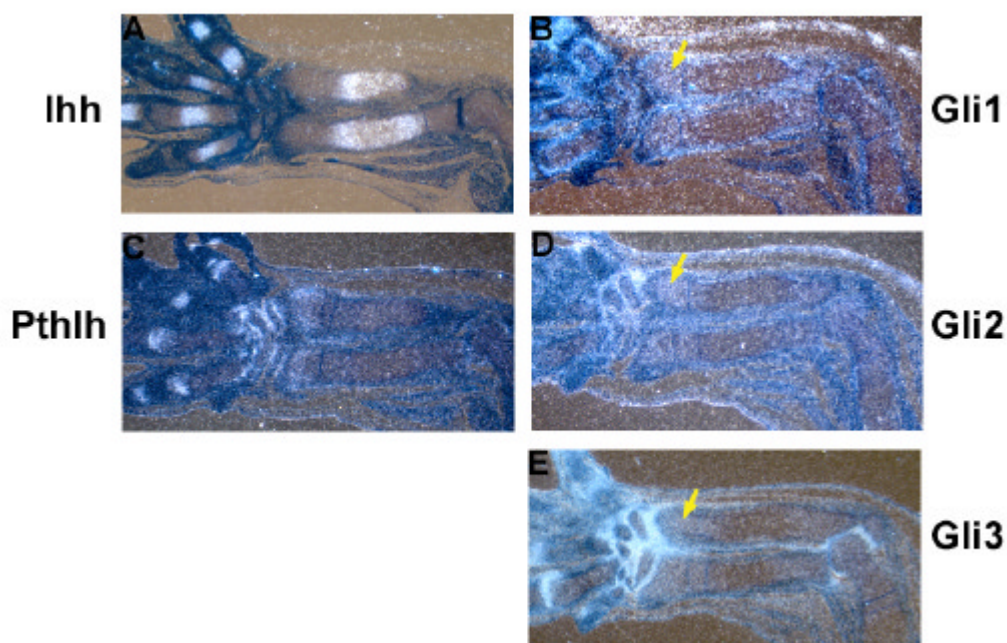


Fig. 25. Expression of the *Gli* gene family. E14.5 wild-type limb sections were hybridized with *Ihh* (A), *Pthlh* (C), *Gli1* (B), *Gli2* (D) and *Gli3* (E) riboprobes. All three *Gli* genes are expressed in the perichondrium and in chondrocytes (yellow arrow in B, D, E). *Gli3* is strongly and *Gli2* weakly expressed in elbow and carpal joints, overlapping with *Pthlh* expression (C).

At E16.5 all three *Gli* genes are expressed in the bone forming region, implicating a redundant function in inducing osteoblast differentiation. Similar as at E14.5, *Gli2* and *Gli3* but not *Gli1* expression is detected in the joint region. Interestingly the expression pattern

of the three *Gli* genes in the chondrocytes are more distinct: *Gli1* is expressed strongest in proliferating chondrocytes flanking the *Ihh* expression domain. In contrast *Gli2* and *Gli3* are strongest expressed in the distal ends of the skeletal elements overlapping with *Pthlh* expression. Towards the *Ihh* expression domain *Gli2* and *Gli3* expression ceases (Fig. 26). Thus all three *Gli* genes are expressed in overlapping but distinct domains in the growth plate.

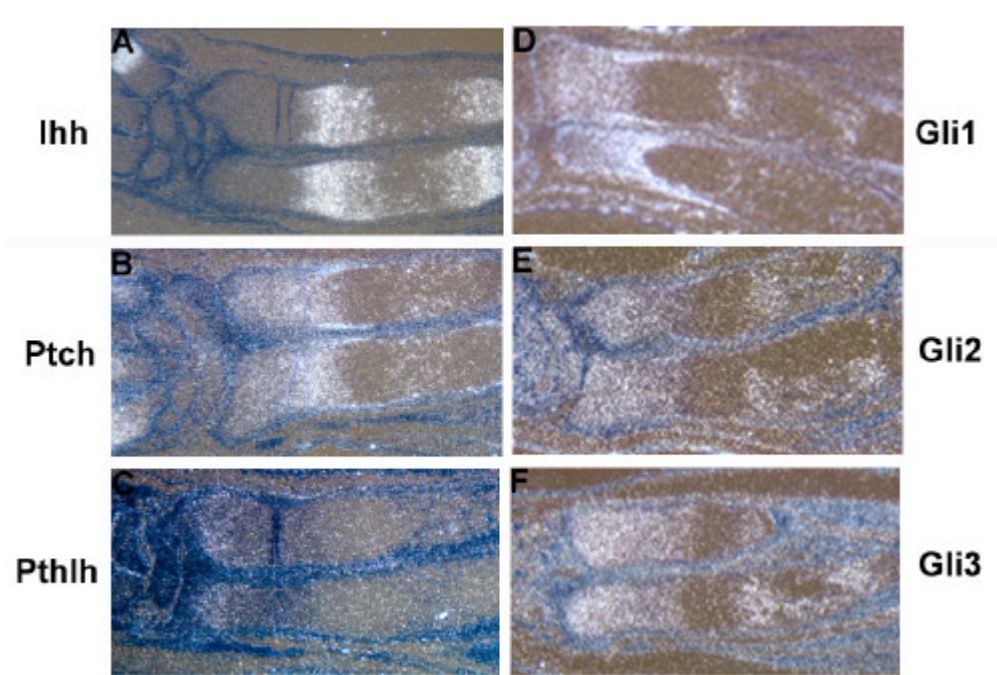


Fig. 26. Expression of the *Gli* gene family in chondrocytes and bone. E16.5 wild-type limb sections were hybridized with with *Ihh* (A), *Ptch* (B), *Pthlh* (C), *Gli1* (D), *Gli2* (E) and *Gli3* (F) riboprobes. *Gli1* is expressed similar to *Ptch* in proliferating chondrocytes flanking the *Ihh* expression domain. *Gli2* expression can be detected in periarticular chondrocytes, overlapping with *Pthlh* expression and weak in proliferating chondrocytes. *Gli3* expression is strongest in the joint region and similar like *Gli2* weaker expression can be detected in periarticular and proliferating chondrocytes. All three *Gli* genes are additionally expressed in the bone forming region.

Analysis of neural tube development revealed that the onset of *Gli2* and *Gli3* expression is independent of Shh signaling, whereas *Gli1* expression is induced by Shh. However, ectopic Shh was shown to negatively regulate the transcription of *Gli3* (Marigo et al., 1996). To investigate, if expression of the *Gli* genes depends on *Ihh* signaling, we studied their expression in *Ihh* deficient mice (Fig. 27). *Gli2* and *Gli3* are expressed in chondrocytes, suggesting that both genes are transcriptionally regulated independent of

Ihh. However *Gli1* expression is not detectable in *Ihh* deficient limbs. This indicates that similar as in the neural tube, *Gli1* expression is dependent on the activator forms of *Gli2* or *Gli3*.

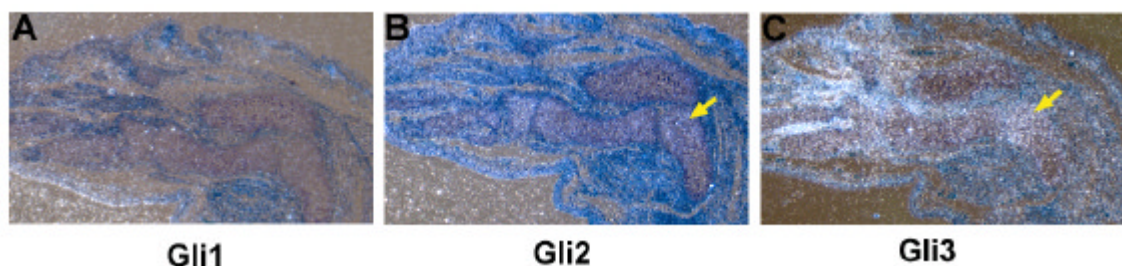


Fig. 27. Expression of *Gli* genes in *Ihh* deficient mice. Limbs of E16.5 *Ihh* deficient mice were hybridized with *Gli1* (A), *Gli2* (B) and *Gli3* (C) riboprobes. *Gli2* and *Gli3* are expressed in chondrocytes (yellow arrow in B and D) and *Gli3* is additionally expressed in the joint region. No expression of *Gli1* can be detected (A).

5.12 Analysis of *Gli3* mutant mice

A naturally occurring mouse mutation of *Gli3*, ‘*Extra toes*’ was first described by Johnson in 1967 (Johnson, 1967). Null mutations of *Gli3* cause severe craniofacial abnormalities and a strong autopod phenotype (Hui and Joyner, 1993). In *Gli3* mutants, the fore limbs exhibit a severe polydactyly (seven to eight digits) and humerus, ulna and radius are slightly shortened (Mo et al., 1997). However, chondrocyte differentiation in these mice has not been analysed on a molecular level. To characterize *Gli3* mutant mice, we analysed the expression of several chondrocyte markers at E14.5 and E16.5. At E14.5 the two domains of *Ihh* expression have not segregated at the same rate as in wild-type limbs, indicating a general delay in endochondral ossification (Fig. 28 A, B). Interestingly expression of *Pthlh* is slightly upregulated in *Gli3*^{-/-} mutants at this stage.

At E16.5 a mild delay in endochondral ossification in *Gli3*^{-/-} mice is clearly visible. Radius and ulna are shorter than in wild-type limbs and the zone of ossification in the center of skeletal elements is reduced (Fig. 28 I, J blue arrow). Comparing the distance between the expression domain of *Ihh* and the end of the skeletal elements in radius of *Gli3*^{-/-} and wild-type mice revealed that the zone of proliferating chondrocytes is slightly shortened in *Gli3*^{-/-} mutants (Fig. 28 E, F, red arrow). A reduced zone of proliferating

chondrocytes implicates that the onset of hypertrophic differentiation is accelerated. However at E14.5 we observed slightly upregulated levels of *Pthlh* expression, which normally leads to a delay of hypertrophic differentiation. In addition, the size of the *Ihh* expression domain is unchanged. To analyse if altered transcription levels of *Pthr1* or disturbed *Ihh* signaling may account for the accelerated onset of hypertrophic differentiation, we hybridized riboprobes for *Pthr1* and *Ptch*. We could not detect any striking difference in the expression pattern of these genes (Fig. 28 G-J).

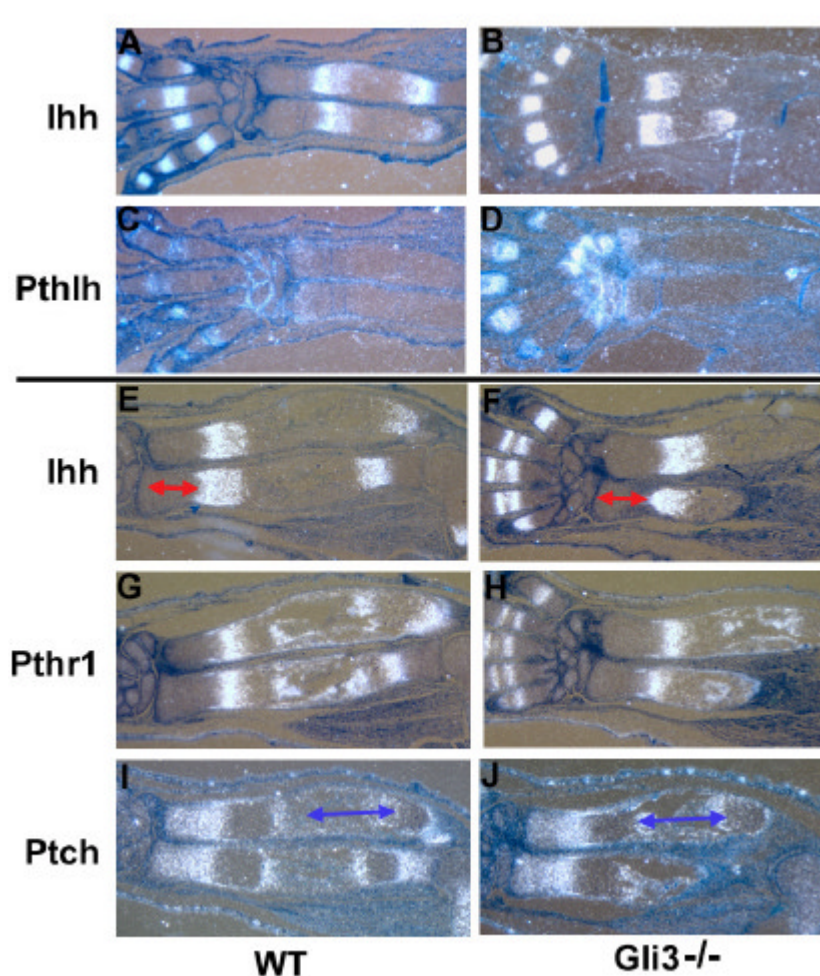


Fig. 28. Characterization of *Gli3*^{-/-} mice. *In situ* hybridisation of E14.5 (A-D) and E16.5 (E-J) wild-type and *Gli3*^{-/-} limb sections. (A-D). At E14.5 ulna and radius are shorter than wild-type litter mates and the separation of the two domains of *Ihh* expression is delayed. *Pthlh* expression is slightly upregulated in *Gli3*^{-/-} mice (D). (E-J) At E16.5 radius and ulna of *Gli3*^{-/-} mutants display a reduced zone of proliferating chondrocytes (red arrow, E, F). The zone of ossification in the center of the skeletal elements is reduced (blue arrow, I, J). No changes in the expression pattern of *Pthr1* and *Ptch* can be detected in *Gli3*^{-/-} limbs (G-J).

The zone of proliferating chondrocytes can be subdivided in two zones: a smaller zone of periarticular chondrocytes at the distal end of the skeletal elements (zone I) and the zone of columnar chondrocytes (zone II) (see 2.9). *Fgfr1* is expressed in periarticular and in hypertrophic chondrocytes, whereas *Fgfr3* is expressed in columnar and prehypertrophic chondrocytes (Minina et al., submitted). To investigate if the region of periarticular or columnar chondrocytes is affected in *Gli3* mutant mice, we analysed the expression of *Fgfr1* and *Fgfr3* (Fig. 29). Interestingly the domain of *Fgfr1* expression is reduced in *Gli3*^{-/-} mice (Fig. 29 C, D), whereas the expression pattern of *Fgfr3* is unchanged (data not shown). As the reduced expression domain of *Fgfr1* points to a reduced domain of periarticular chondrocytes, we reinvestigated the expression of *Pthlh*, which is expressed in a subpopulation of these cells (Fig. 29 E, F). We observed a shift of *Pthlh* expression (blue line in Fig. 29 E, F) towards the end of the skeletal elements (red line in Fig. 29 E, F). We next measured the distance between the end of the *Pthlh* expression domain and the beginning of the *Ihh* expressing domain (Fig. 29) and found that this distance is of similar size in *Gli3*^{-/-} and wild-type embryos (yellow arrow in Fig. 29 E, F, n=2). Therefore the *Pthlh* induced onset of hypertrophic differentiation is not accelerated in *Gli3*^{-/-} mice. These results suggest that differentiation of distal periarticular chondrocytes into columnar chondrocytes is regulated by *Gli3*.

5.13 Interaction of *Ihh* and *Gli3*

Ihh deficient mice do not express *Pthlh*. They are characterized by severely reduced chondrocyte proliferation, an accelerated onset of hypertrophic differentiation and lack of ossification in endochondral bones. In addition hypertrophic differentiation is not initiated perpendicular to the longitudinal axis of the cartilage elements but starts in their center spreading into all directions (Fig. 30 B, F). The resulting skeletal elements at E16.5 thus display a central hypertrophic region expressing *Col10a1* that is surrounded by non-hypertrophic cells expressing *Col2a1* (Karp et al., 2000; St-Jacques et al., 1999). As described above *Gli3* mutant mice display only a mild bone phenotype.

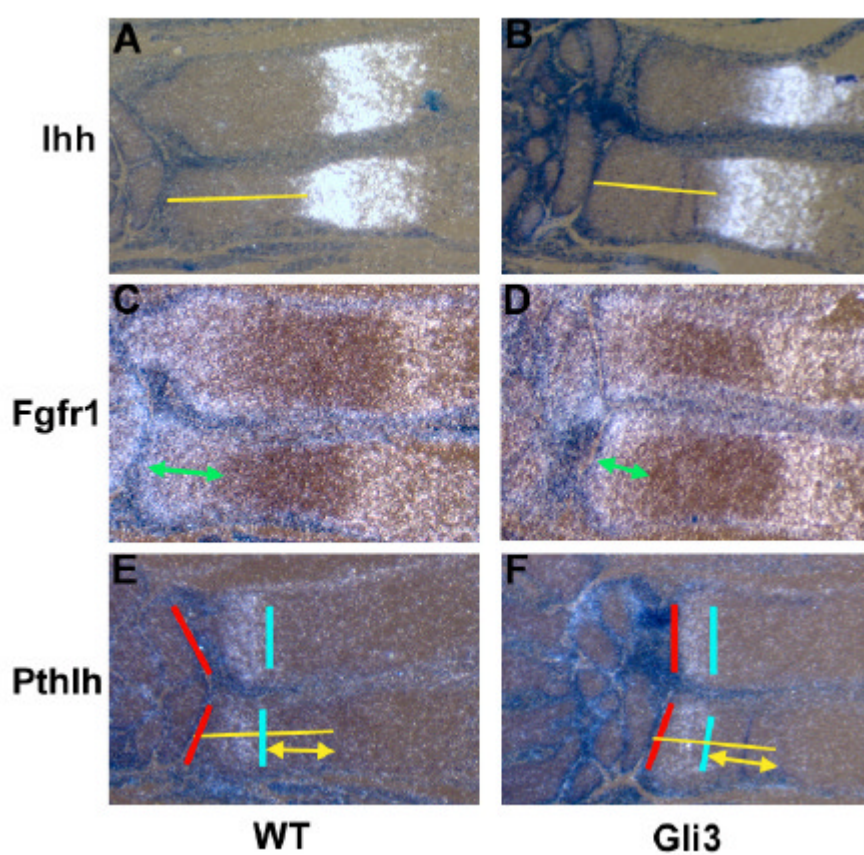


Fig. 29. The zone of periarticular chondrocytes is reduced in *Gli3*^{-/-} mice. (A-F) E16.5 wild-type and *Gli3*^{-/-} limbs were hybridized with riboprobes as indicated. (C, D) The zone of *Fgfr1* expression, a marker for periarticular chondrocytes, is reduced in *Gli3*^{-/-} mice. (E, F, green arrow). Careful analysis of *Pthlh* expression revealed that the expression domain of *Pthlh* (end of domain is demarcated by the blue bar) is shifted towards the end of radius and ulna in *Gli3*^{-/-} mice compared to wild-type (red bar). The distance between the end of the *Pthlh* expression domain and the beginning of the *Ihh* expression domain (measured with the yellow bar) is of similar size in wild-type and *Gli3*^{-/-} limbs (yellow arrow, n=2).

To investigate the potential interaction between *Ihh* and *Gli3* we generated compound mutants of these two genes. Interestingly, analysis of *Ihh*^{-/-};*Gli3*^{-/-} double mutants revealed a partial rescue of the *Ihh*^{-/-} phenotype: Cartilage elements are increased in size and display a delay in hypertrophic differentiation of chondrocytes. Strikingly the hypertrophic region develops perpendicular to the longitudinal axis of the bone (Fig. 30 and Fig. 31 A, B). In wild-type limbs the bone collar usually forms adjacent to the hypertrophic chondrocytes and ossification starts at the begin of hypertrophic differentiation. In *Ihh*^{-/-}; *Gli3*^{-/-} skeletal elements, however, no bone collar adjacent to the hypertrophic zone is formed at E16.5 (Fig. 30 D). Strikingly the morphology and orientation of proliferating chondrocytes is

nearly perfectly restored. The zone of periarticular chondrocytes is reduced, however the zone of columnar chondrocytes is of similar size as in wild-type mice (Fig. 31 C, D). The loss of *Gli3* in *Ihh*^{-/-} mice therefore rescues two aspects of chondrocyte differentiation: chondrocyte proliferation and the onset of hypertrophic differentiation. However, *Gli3* does not seem to regulate bone collar formation, indicating that this process is dependent on activating function of *Gli* genes rather than loss of repression.

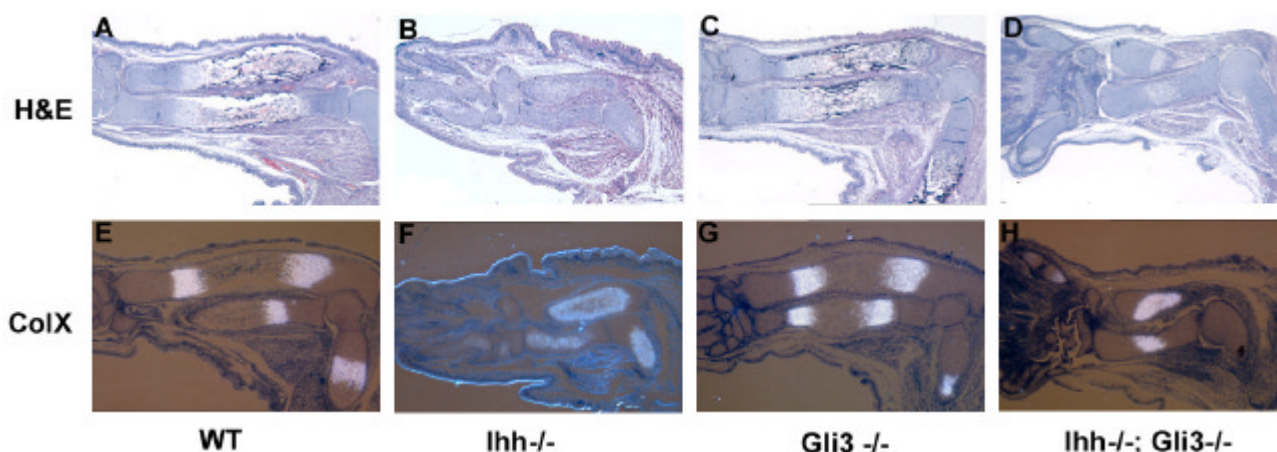


Fig. 30. Interaction of *Ihh* and *Gli3*. (A-D) Hematoxylin/Eosin staining of E16.5 wild-type (A), *Ihh*^{-/-} (B), *Gli3*^{-/-} (C) and *Ihh*^{-/-};*Gli3*^{-/-} (D) mice. The severe bone phenotype of *Ihh*^{-/-} mice (B) is rescued by loss of *Gli3* function (D). (D) Radius and ulna of *Ihh*^{-/-};*Gli3*^{-/-} mice display distinct zones of proliferating and hypertrophic chondrocytes and the size of the skeletal elements are increased compared to *Ihh*^{-/-} mice (B). No bone formation is detected in *Ihh*^{-/-};*Gli3*^{-/-} limbs. (E-H) *In situ* hybridization with *Col10a1* riboprobe demarcates a distinct zone of hypertrophic chondrocytes in the center of radius and ulna in *Ihh*^{-/-};*Gli3*^{-/-} limbs, compared to an irregular and broadened zone of hypertrophic cells in *Ihh*^{-/-} limbs (F).

To investigate the rescued chondrocyte proliferation and the onset of hypertrophic differentiation, we performed *in situ* hybridization, to analyse the expression of *Ihh* target genes *Ptch* and *Pthlh* (Fig. 32). Both genes are not expressed in limbs of *Ihh* deficient mice. Importantly low levels of *Pthlh* expression are detectable in the joint region (Fig. 32 H) and are most likely responsible for the delayed onset of hypertrophic differentiation in *Ihh*^{-/-};*Gli3*^{-/-} double mutants.

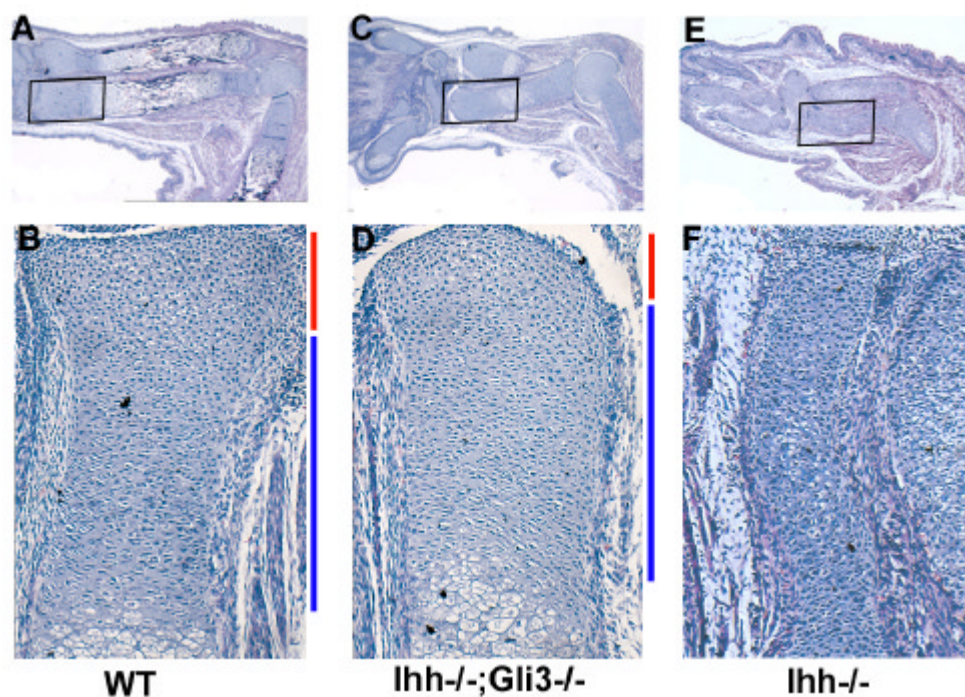


Fig. 31. Chondrocyte organization is rescued in *Ihh*^{-/-};*Gli3*^{-/-} compound mutants. (A-F) Hematoxylin/Eosin staining of wild-type (A, B), *Ihh*^{-/-};*Gli3*^{-/-} (C, D) and *Ihh*^{-/-} (E, F) limbs. (B, D, F) Magnification of the zone of proliferating chondrocytes from insets in (A, C, E). The zone of round, periarticular chondrocytes in *Ihh*^{-/-};*Gli3*^{-/-} mice is reduced (red bar), whereas the zone of columnar chondrocytes is of similar size (blue bar) compared to wild-type limbs.

In addition *Ptch* expression can be detected at low levels in proliferating chondrocytes of *Ihh*^{-/-};*Gli3*^{-/-} mice. Therefore the slightly elevated *Pthlh* levels in *Gli3*^{-/-} mice and the restored *Pthlh* expression in *Ihh*^{-/-};*Gli3*^{-/-} mice suggest that *Pthlh* is one transcriptional target of the *Gli3* repressor.

In summary these data strongly suggest that *Gli3* acts mainly as a repressor downstream of *Ihh* signaling, controlling the onset of hypertrophic differentiation by repressing the expression of *Pthlh* and by repressing chondrocyte proliferation.

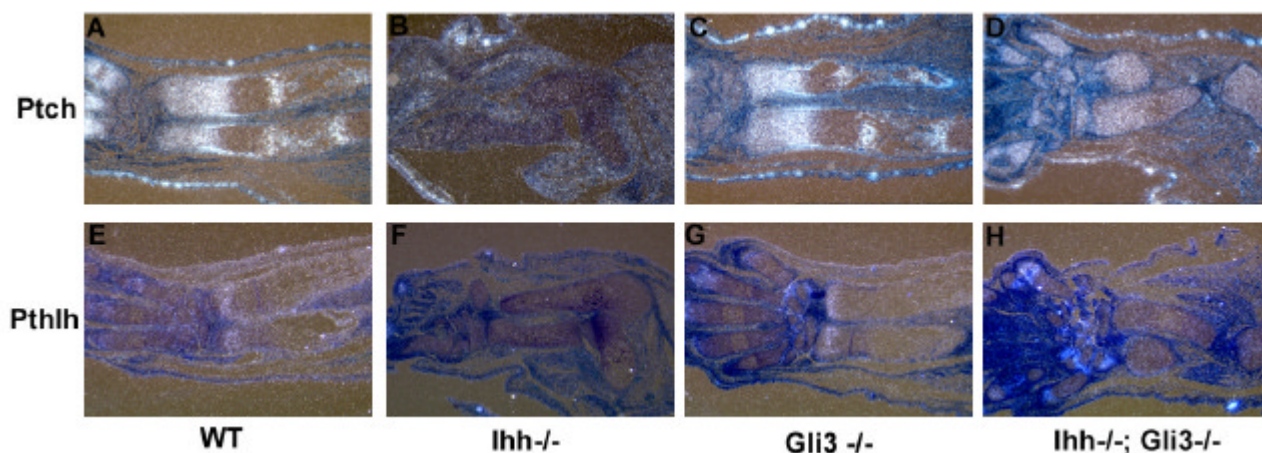


Fig. 32. Loss of *Gli3* in *Ihh* deficient mice rescues expression of *Ihh* target genes *Ptch* and *Pthlh*. E16.5 wild-type (A, E), *Ihh*^{-/-} (B, F), *Gli3*^{-/-} (C, G) and *Ihh*^{-/-};*Gli3*^{-/-} (D, H) mice were hybridized with *Ptch* (A-D) and *Pthlh* (E-F) riboprobes. (A-D) Low levels of *Ptch* are expressed in *Ihh*^{-/-};*Gli3*^{-/-} limbs (D), compared to normal levels of expression in wild-type (A) and *Gli3*^{-/-} mice (C) and no expression in *Ihh*^{-/-} mice (B). (E-H) *In situ* hybridization with a *Pthlh* riboprobe reveals normal levels of expression in wild-type (E), no expression in *Ihh*^{-/-} (F), slightly elevated expression in *Gli3*^{-/-} (G) and low levels of expression in the joints of *Ihh*^{-/-};*Gli3*^{-/-} limbs.